Instruments and Methods

New LA-ICP-MS cryocell and calibration technique for sub-millimeter analysis of ice cores

Sharon B. SNEED,[1,2] Paul A. MAYEWSKI,[1,2] W.G. SAYRE,[1] Michael J. HANDLEY,[1] Andrei V. KURBATOV,[1,2] Kendrick C. TAYLOR,[3] Pascal BOHLEBER,[1,4] Dietmar WAGENBACH,[4] Tobias ERHARDT,[5] Nicole E. SPAULDING[1]

[1]*Climate Change Institute, University of Maine, Orono, ME, USA*
[2]*School of Earth and Climate Sciences, University of Maine, Orono, ME, USA*
[3]*Desert Research Institute, Nevada System of Higher Education, Reno, NV, USA*
[4]*Institute of Environmental Physics, University of Heidelberg, Germany*
[5]*Oeschger Center for Climate Change Research and Institute for Climate and Environmental Physics, University of Bern, Bern, Switzerland*
Correspondence: Sharon B. Sneed <sharon.sneed@maine.edu>

ABSTRACT. Ice cores provide a robust reconstruction of past climate. However, development of timescales by annual-layer counting, essential to detailed climate reconstruction and interpretation, on ice cores collected at low-accumulation sites or in regions of compressed ice, is problematic due to closely spaced layers. Ice-core analysis by laser ablation–inductively coupled plasma–mass spectrometry (LA-ICP-MS) provides sub-millimeter-scale sampling resolution (on the order of 100 μm in this study) and the low detection limits (ng L^{-1}) necessary to measure the chemical constituents preserved in ice cores. We present a newly developed cryocell that can hold a 1 m long section of ice core, and an alternative strategy for calibration. Using ice-core samples from central Greenland, we demonstrate the repeatability of multiple ablation passes, highlight the improved sampling resolution, verify the calibration technique and identify annual layers in the chemical profile in a deep section of an ice core where annual layers have not previously been identified using chemistry. In addition, using sections of cores from the Swiss/Italian Alps we illustrate the relationship between Ca, Na and Fe and particle concentration and conductivity, and validate the LA-ICP-MS Ca profile through a direct comparison with continuous flow analysis results.

KEYWORDS: ice core, snow and ice chemistry

INTRODUCTION

Ice-core proxies for past atmospheric circulation patterns (Mayewski and others, 1997), sea-ice extent (O'Dwyer and others, 2000), snow accumulation rates (Meese and others, 1994; Kaspari and others, 2004), pollution histories (Wagenbach and others, 1988) and volcanic eruptions (Hammer and others, 1981; Zielinski and others, 1996) have all been developed through a variety of chemical analytical techniques. These techniques include ion chromatography (IC), gas chromatography, continuous flow analysis (CFA), stable-isotope mass spectrometry and elemental analysis. When plotted against depth/age of the ice core the chemical profiles determined by these measurements reveal sub-annual patterns attributable to source region, source strength, transport mechanism, deposition and atmospheric circulation patterns. The current highest-resolution sampling is ~1 cm by CFA (Bigler and others, 2011) and continuous melting (e.g. Osterberg and others, 2006). Therefore, examination of seasonal cycles in the chemistry records of ice cores collected from low-accumulation sites and from highly compressed core sections is not possible using current methods. Laser ablation offers a technique with the ultra-high sampling resolution necessary under these conditions to be used as a complementary tool for climate reconstruction together with more traditional analytical methods.

Sampling of solid materials using laser ablation (LA) began in the 1960s (Miller, 1993), and the first elemental measurement of ablated material by inductively coupled plasma–mass spectrometry (ICP-MS) was carried out by Gray (1985). As a consequence LA-ICP-MS has become an important and constantly evolving environmental, geological, archeological, nuclear and biological sampling and analysis tool (Russo and others, 2002). Typical components of a LA system include a laser with adjustable spot size and viewing and positioning capabilities, and an airtight ablation chamber fitted with an optical window including inlet and outlet ports to collect and transport ablated material to the ICP-MS using either He or Ar through Teflon tubing.

Lasers used in LA applications are either solid-state or gas-based and the choice of laser output wavelength is based on the material to be ablated, ease of operation, required maintenance and initial and operational costs (Longerich, 2008). The fundamental wavelength for Nd:YAG (neodymium-doped yttrium aluminum garnet) solid-state lasers is 1064 nm and this can be frequency-multiplied to generate outputs of 266, 213 and 193 nm that are commonly utilized in ablation work (Longerich, 2008). Gas-based, or eximer,

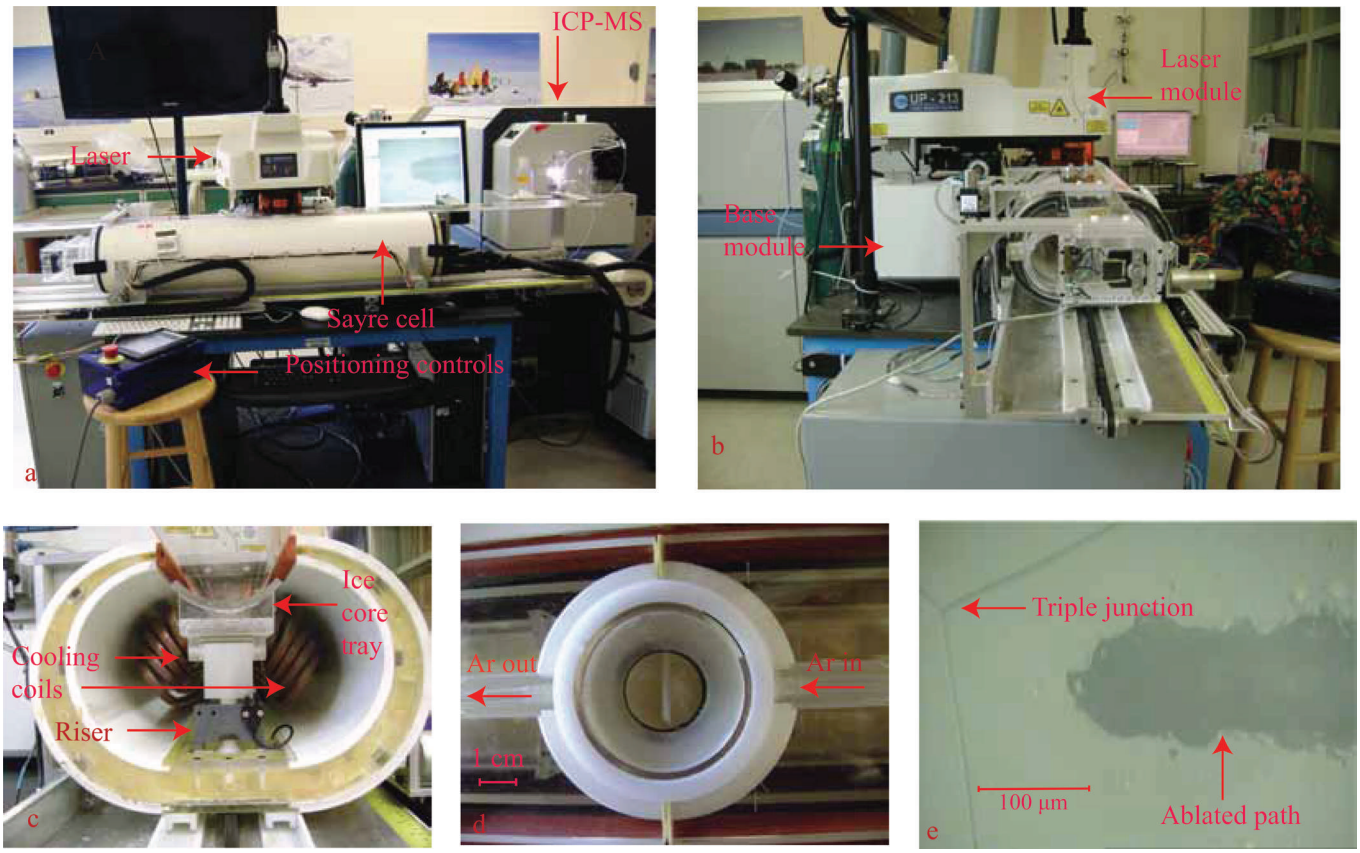

Fig. 1. (a) Complete Sayre Cell™ system. Cryocell moves left and right under the fixed upper rail on Teflon rails using a Kevlar belt. The ablation chamber is fixed in place under the laser, which moves in the *x* and *y* directions. (b) Side view of LA system. Upper laser module moves during the ablation pass; ice in the Sayre Cell™ is stationary. (c) End view into the cryocell. The ice core is placed in the tray, and two risers position it up to the ablation chamber. Cooling coils run the length of the cryocell on both sides from the recirculating chiller. (d) Top view of ablation chamber positioned in center of fixed upper rail of cryocell. Wavelength-specific window held in place with an o-ring and a c-ring to create an airtight seal formed as bottom gasket contacts the ice surface. (e) Image of ablated pass on an ice sample. Triple junction can be seen in the surface.

laser output is 193 nm for an argon–fluoride mixture. Eximer-type lasers require a supply of argon and fluorine gases but do not use frequency-multiplying crystals that require periodic maintenance (Longerich, 2008).

Ablation chambers can be of closed or open design. A closed chamber contains the sample within its interior and is generally used for smaller samples. For larger samples, or samples that cannot be subsectioned, an open cell is used. The base of the open cell must have an airtight seal with the sample. The size of the chamber, along with gas flow rate, determines the time required to remove the ablated material (washout time). To conduct ice-core analysis by LA also requires a device to maintain the sample at below-freezing temperatures.

In the early 2000s Reinhardt and others (2001, 2003) pioneered the application of LA-ICP-MS for ice-core analysis. They used a 1064 nm solid-state laser and achieved a spatial resolution of ~300 μm. Ice-core samples were cut into 10 cm × 1 cm disks or 10 cm × 5 cm segments. Multiple elements were measured by ICP-MS, and the resulting intensities (counts s^{-1}) were converted to concentration by calibration curves constructed from lasing frozen standards. The temperature of their closed-style ablation chamber was maintained at –30°C by a cooler circulating silicon oil, however, because the volume of the chamber was large enough to hold 10 cm samples; washout time was ~7 min. Recent work has reduced the washout time of large ablation chambers to ~1 s per order-of-magnitude ICP-MS measured intensity by incorporating a small, funnel-shaped inner cell to minimize the volume into which the sample is collected (Müller and others, 2009). Using this ablation chamber, cooled by Peltier elements, Müller and others (2011) ablated ice (cut into 50 mm × 13 mm × 12 mm strips) with a 193 nm eximer laser and a spot size of 280 μm. With funding from the W.M. Keck Foundation, we have built upon the foregoing studies to reduce sample preparation time and effort, to further refine sample resolution, and to simplify the calibration between intensity and concentration.

To validate these advances we chose to measure Ca, Na and Fe by LA-ICP-MS in specifically selected ice-core samples to investigate the degree of repeatability, the potential for discerning annual layers in the chemical record of highly compressed core sections and the similarity between profiles determined by this method and other high-resolution methods commonly used in ice-core research.

METHODS

Set-up

We designed our new cryocell, named the Sayre Cell™ (Fig. 1a–d), to hold up to a 1 m length of ice core at below-freezing temperatures (–25°C) and have the necessary small-volume (~20 cm^3) open-design ablation chamber. The entire

system, including the ICP-MS, laser and Sayre Cell, is part of the Keck Laser Ice Facility at the Climate Change Institute, University of Maine. The Sayre Cell has Plexiglas ribs that join the inside and outside shells of PVC piping. The interstitial spaces are filled with spray foam insulation and it moves in the horizontal direction under a fixed upper rail (Fig. 1c). A PTFE ablation chamber is centered in the stationary upper rail. The top of the chamber (Fig. 1d) contains a round laser-compatible optical window 5 cm in diameter, and the bottom opening is ringed with compressible gasket material (closed cell foam). We constructed three chambers, with the same size and shape but different bottom openings, to be used with cores of various widths ranging from 3 to 8 cm. The same chamber is used within each experiment. Bottom openings are either 5 or 2.5 cm circles or a 4.5 cm × 1.5 cm oval. When necessary, we flow-dry N_2 across the top window to remove condensation. Risers move the core in the vertical direction to establish a seal with the ablation chamber. There are inlet and outlet ports at opposite sides of the ablation chamber for the argon carrier gas that feeds into the ICP-MS. Transport of the sample aerosol to the ICP-MS occurs in ~8 s. Cooling is achieved through a Neslab RTE40 recirculating chiller connected at the right-end cap to 1 m long coils of copper tubing positioned along either side of the cell. A fan is mounted onto the left-end cap to provide a uniform temperature of –25°C. The entire cell system is positioned under a New Wave UP-213 laser (original ablation chamber removed) and connected to a Thermo Element 2 ICP-MS with Teflon tubing. Although ice is transparent to radiation at 213 nm (Warren and Brandt, 2008), the high power density of the laser pulse makes it possible to ablate transparent material (Tadano and others, 2004). The 213 nm wavelength is the fifth harmonic of a 1064 nm Nd:YAG laser. We chose a laser at this wavelength for three reasons: (1) At 213 nm wavelength the laser is absorbed by a wide range of materials (Longerich, 2008). (2) The beam is adjustable to spot sizes of 4–100 μm, making it suitable for ice as well as particles. (3) Fewer large particles of ablated material are produced at shorter wavelengths, improving the stability of the signal (Guillong and others, 2003). The UP-213 is equipped with aperture imaging for spot size determination and optical magnification of 5.6× to 36×. The upper laser module, called Floating Platform by New Wave, is moveable at 52 mm in the *x* and *y* directions at 1 μm resolution. We have included a video capture component in the laser system for post-acquisition examination of ice structure compared with chemical profiles.

Operation

In order to develop LA-generated profiles at sub-millimeter sample resolution, we have chosen, thus far, to measure the elements individually using line scans. In addition to ultra-high resolution, line scanning produces a continuous profile along the length of the ice sample. After the cut surface of the ice is cleaned using a ceramic scraper, selected elements are measured down the length of the core section using 100 μm diameter laser spots rapidly fired to form ablated parallel lines measuring each element. Lines are separated by 200 μm to avoid overlap of the ablated surface. Once all elements are analyzed, the core is lowered away from the ablation chamber, the Sayre Cell moved automatically 2 or 4 cm horizontally, depending on the bottom opening of the ablation chamber, and the ice is raised under the chamber. To prevent air from entering the ICP-MS, the gas flow is switched to bypass using the laser mass-flow controllers before lowering the ice. Upon repositioning, the gas flow is set to purge for 2 min, then returns to online. Soundness of the seal is tested in two ways: (1) A flowmeter is built into the cryocell system. It may be switched between in-line (to measure the Ar flow) and offline (to permit gas flow to the ICP-MS). (2) The ICP-MS is tuned with the ice in place, so even a small leak would be observable in the signal. The next 2 cm segment is started precisely at the end of the previous scan lines. An image of an ablated line appears in Figure 1e. The LA system is electronically interfaced such that the laser triggers the ICP-MS to begin analysis. For our experiments thus far, the ICP-MS software is configured to collect 500 data points in each 1 cm (2 min) line segment. Sampling resolution is determined by the laser spot diameter, firing rate, scan speed and ICP-MS sampling rate. Table 1 contains the settings used in these experiments. The laser fires a 100 μm spot at 20 Hz (20 firing s^{-1}) and moves at 85 μm s^{-1} or 4.25 μm $firing^{-1}$. The ICP-MS collects one sample every 0.25 s or 5 firing s^{-1}. Thus sampling resolution is 100 μm + (4.25 μm $firing^{-1}$ × 5 firing $sample^{-1}$), or 121.25 μm $sample^{-1}$, along the length (depth) of the ice core.

Calibration

The ICP-MS is fitted with a dual cyclonic spray chamber with entrance ports for both liquid samples and laser aerosols (Elemental Scientific, USA). The Elemental Scientific low-flow nebulizer (20 μL min^{-1}) is designed to reduce the amount of liquid aspirated and to facilitate higher laser ablation chamber gas flows. Dual liquid and laser entrance ports make it possible to introduce daily tune solution and liquid standards to the ICP-MS without changing the sample introduction system. Thus, calibration can be completed using a combination of liquid standards and frozen reference materials. The calibration procedure is in two steps. First, three or four liquid standards, at concentrations that bracket the expected concentrations of the samples, are measured to construct calibration equations for chosen elements. Relative standard deviations (RSD) of the liquid standard measurements were 3.3%, 1.4% and 2.9% for Ca, Na and Fe respectively. Second, we ablate frozen river water reference material for trace metals, SLRS-5 (National Research Council Canada), to establish a transfer function to relate liquid measurements to solid measurements. The SLRS-5 is diluted to 1% to bring the concentrations closer to the expected ice-core values. Preparation of frozen standards can be problematic due to inhomogeneous freezing of ionic solutions. Reinhardt and others (2001) used flash freezing to prepare standards; however, we chose to freeze in a stepwise manner to minimize inhomogeneities. A 75 mm Petri dish is partially filled with standard and allowed to freeze on an Anti-Griddle (PolyScience, USA) at ~–34°C in a class 100 clean room. More SLRS-5 is added and allowed to freeze. Finally, a very thin top layer of SLRS-5, ~1 mm thick, is added and frozen. Three 1 cm ablated lines (measured over 137 s) are lased in frozen SLRS-5 and the total counts s^{-1} (cps) for each element averaged to further remove inhomogeneities. An example is presented in Figure 2, with average RSDs along the length of the ablation line of 24%, 24% and 23% for Ca, Na and Fe respectively. This average response is used to calculate the concentration from the liquid calibration equation. The ratio of the certified SLRS-5 concentrations (10.5 ± 0.4 μg g^{-1}, 5.38 ± 0.10 μg g^{-1} and 91.2 ± 5.8 μg kg^{-1} for Ca, Na and Fe

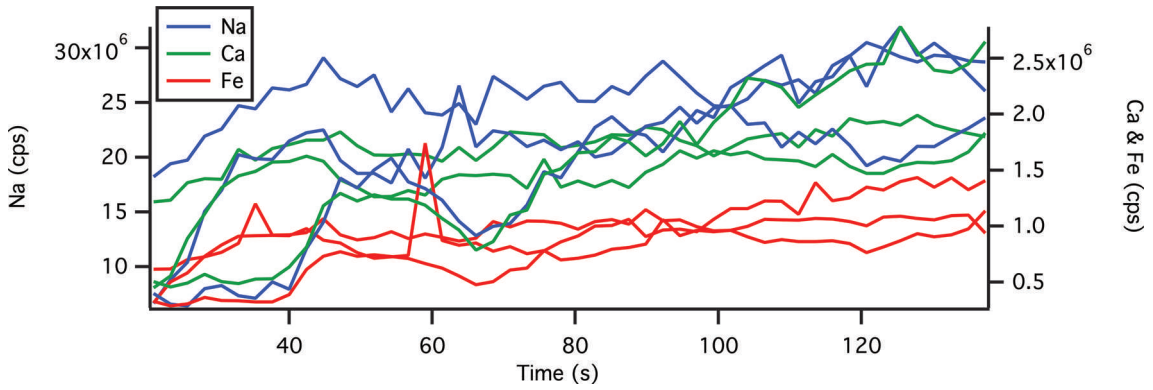

Fig. 2. Multiple ablation passes in different areas of frozen standard reference material SLRS-5 Ca (green), Na (blue) and Fe (red). Take-up time is not included. Variability in the signal is due to inhomogeneities in the frozen standard.

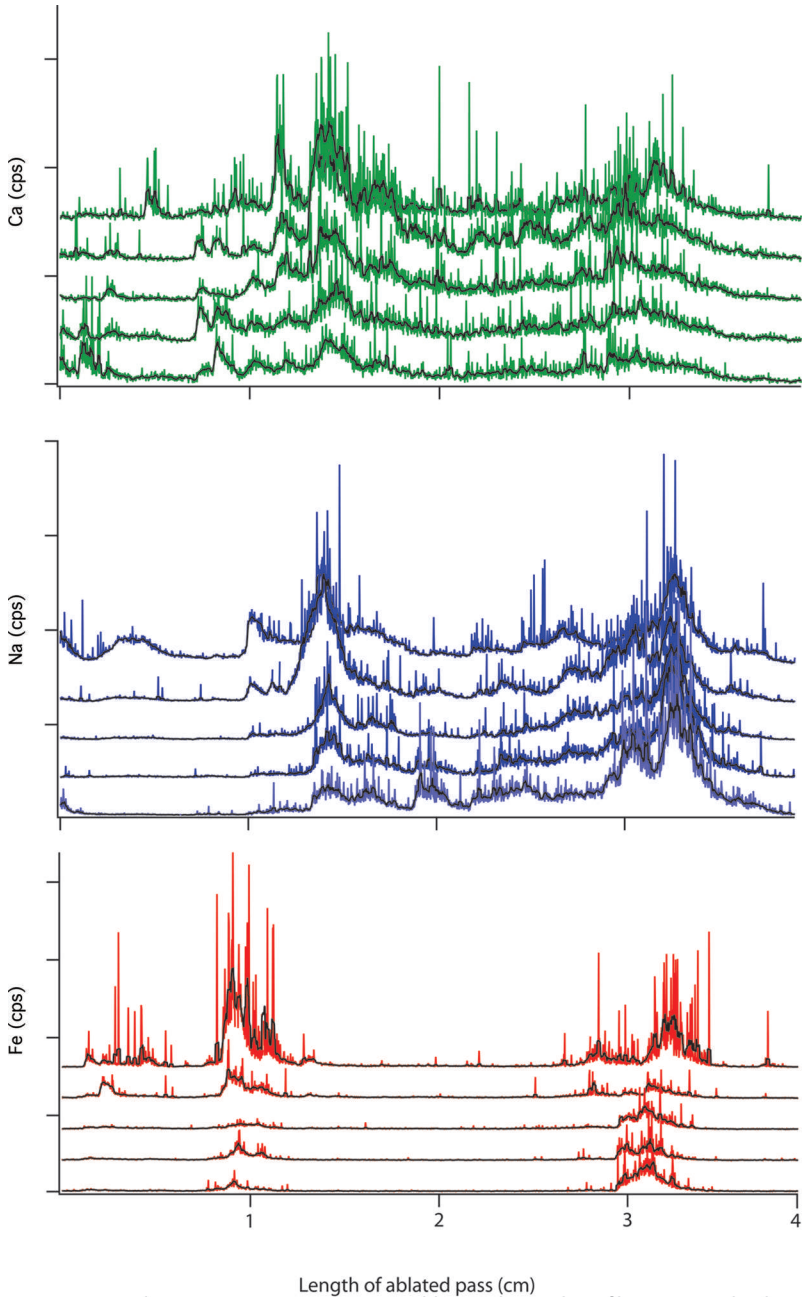

Fig. 3. Replicate LA-ICP-MS Ca, (green), Na (blue) and Fe (red) profiles in a Greenland ice core, each obtained in the same line. Subsequent ablation pass is 10 μm deeper. Average raw correlations are 0.78, 0.58 and 0.54, and 0.81, 0.88 and 0.75 on smoothed data, for Ca, Na and Fe respectively.

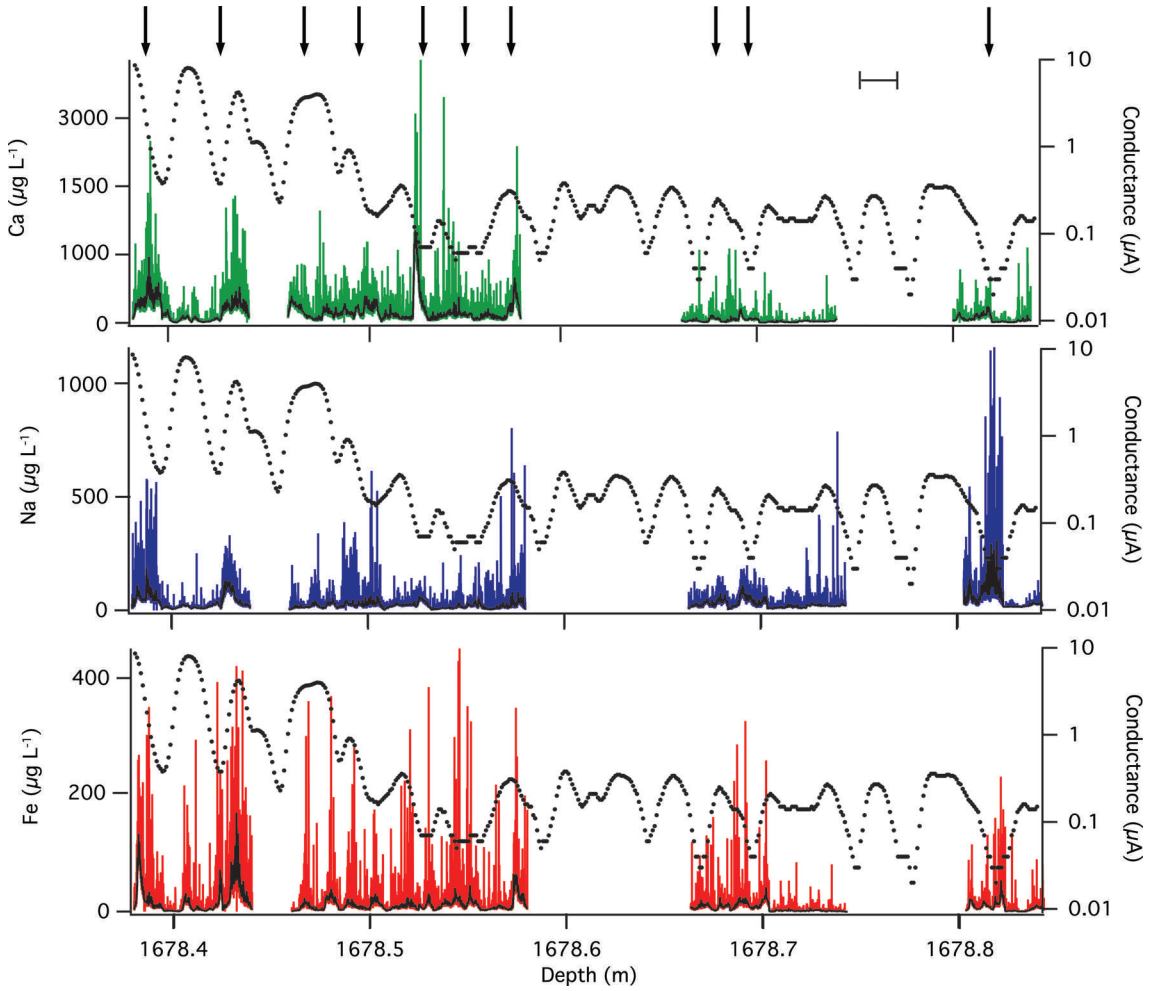

Fig. 4. Raw Ca (green), Na (blue) and Fe (red) concentrations measured using the LA-ICP-MS system on the GISP2 ice core in meter 1678. The mean ten-point smoothed profile of each is included (black curve). Black dotted profile is of the original electrical conductivity measurements. Arrows indicate annual layers as determined using maximum Na peaks in the LA-ICP-MS profiles. Error bar represents combined depth error estimates for LA-ICP-MS (±0.5 cm) and GISP2 ECM (±0.5 cm). LA-ICP-MS detection limits are 2.1, 2.3 and 0.1 μg L^{-1} for Ca, Na and Fe respectively, and analytical error estimates are a few percent for ECM.

respectively) to the calculated concentration results in a transfer function to convert ablated results to concentrations. This calibration strategy assumes a constant volume of ablated material. System detection limits were calculated using 3σ of ten ablation passes on frozen deionized water. Detection limits were determined at 2.1, 2.3 and 0.1 μg L^{-1} for Ca, Na and Fe respectively. Limits of quantification ($10\sigma \pm 10\%$) were determined at 7.0 ± 0.7, 7.7 ± 0.8 and 0.3 ± 0.03 μg L^{-1} for Ca, Na and Fe respectively.

LA-ICP-MS parameters are optimized daily; Table 1 shows the respective operating conditions.

RESULTS AND DISCUSSION

Assessing measurement repeatability

To determine if, or how, LA-ICP-MS measurements change with depth of laser penetration, we ablated multiple passes along the same line on a section of the Greenland Ice Sheet Project 2 (GISP2) deep ice core (72.6° N, 38.5° W) which was collected between 1989 and 1993. Archived ice, in 1 m rods of ~3 cm × 3 cm, was obtained from the US National Ice Core Laboratory, Denver, CO. The section analyzed for this test was from 1678 m depth, within the transition between the glacial and interglacial. Five 4 cm long passes, each 10 μm deeper than the previous as controlled by the *z*-parameter included in the laser software, were ablated and analyzed for Ca, Na and Fe. The patterns in measured intensity (cps) for each pass are quite similar (Fig. 3). As a qualitative assessment we calculate correlations (r) between passes for raw and ten-point smoothed data (Table 2). Average raw correlations are 0.78, 0.5 and 0.54, and 0.81, 0.88 and 0.75 on smoothed data, for Ca, Na and Fe respectively. The intensities decrease slightly in the deeper passes, likely due to the aerosol becoming partially trapped within the ablated canal, which is 40 μm deeper than that created during routine analyses.

Annual-layer identification using multiple chemical species

To examine the chemical profile in compressed ice, we chose to study two sections of the GISP2 ice core. Throughout the core, annual layers were originally determined by chemical concentrations and various physical parameters (Meese and others, 1994); however, below 300 m depth, annual chemical signals were not identifiable in the original record due to the large (~10 cm) sampling resolution at this depth and deeper (Meese and others, 1997). We selected a section from the Younger Dryas,

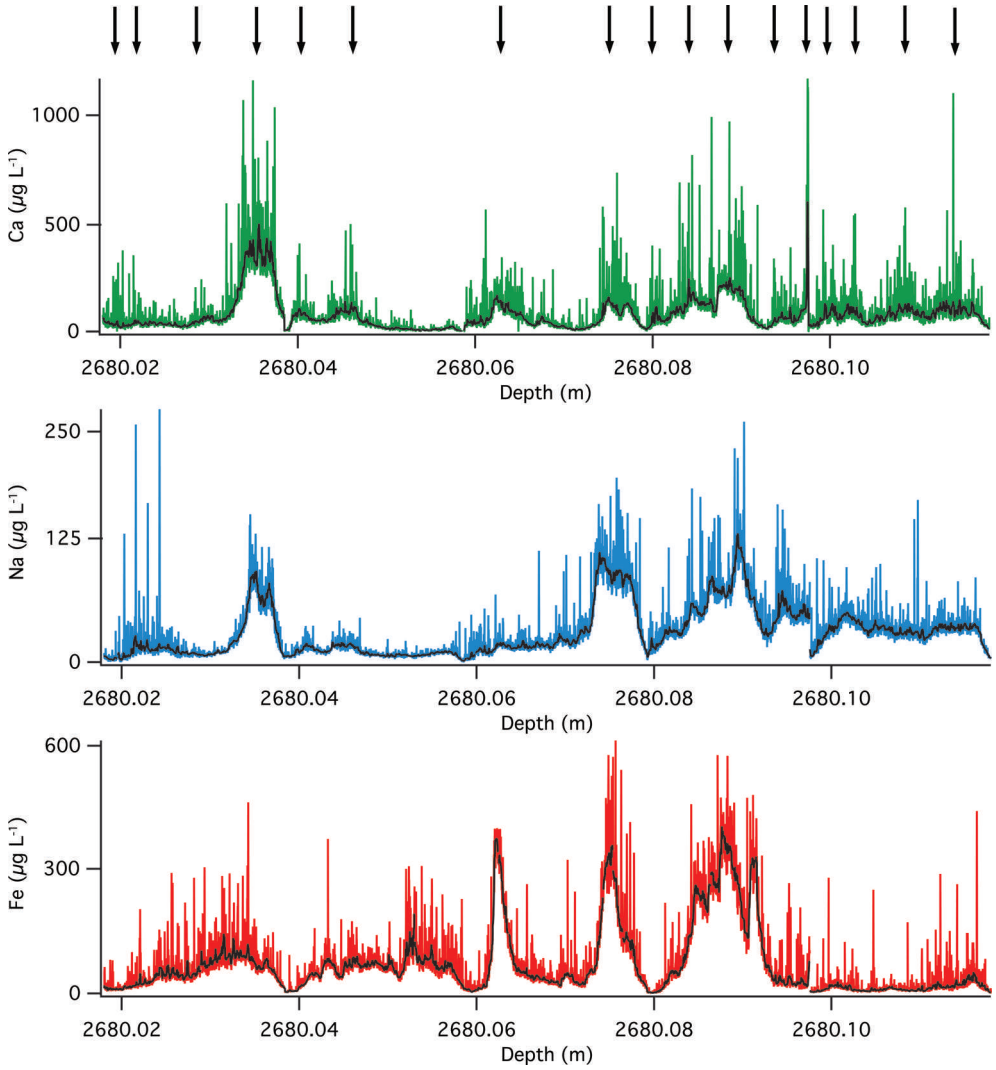

Fig. 5. Raw and smoothed (ten-point running mean) LA-ICP-MS results from GISP2 at 2680 m. Ca (green), Na (blue) and Fe (red). Arrows indicate annual-layer picks based on Na peaks.

1678 m, and one within the glacial period, 2680 m, both below where annual layers were observable in the chemical profile. The original 1678 m section of core was dated by counting layers using visual stratigraphy, electrical conductivity and laser-light scattering (Taylor and others, 1993; Ram and others, 1995; Meese and others, 1997). Visual stratigraphy in the GISP2 ice core was observed as variations in transmitted light that is scattered due to bubbles and grains, recorded on a mm to cm depth scale and then manually grouped to form annual signals (Alley and others, 1997). Electrical d.c. conductivity and laser-light scattering is a measure of seasonally deposited mineral dust, hence the annual signal (Hamilton and Langway, 1967). Direct-current electrical conductivity measurement (ECM) is an indicator of acidity and has a depth resolution of <10 mm (Taylor and others, 1997) and an analytical repeatability of within a few percent (Taylor and others, 1992). ECM is inverse to the dust level due to the neutralizing effect of dust. We ablated 20 cm from meter 1678 and 10 cm from meter 2680 for Ca (dust source), Na (marine source) and Fe (dust source). Raw LA-ICP-MS results of Ca (green), Na (blue) and Fe (red) from meter 1678, with a ten-point running mean included in black, are presented in Figure 4. Breaks and cracks in the 20 year old archived GISP2 ice core coincide with either missing ice sections or sufficiently poor-quality (highly cracked) ice that is too permeable to allow the necessary airtight seal, thus preventing absolutely continuous sampling. Depths of ablated regions were assigned by measuring the distance from the top of the meter section to the start of the ablated lines. Based on a combination of the foregoing physical techniques, there are 33 years of net annual accumulation in meter 1678 (Meese and others, 1997) or ~15 years in 46 cm. Despite missing sections, there is still sufficient continuous sampling to clearly resolve annual signals in the LA-ICP-MS-derived chemical profiles, shown with previously determined ECM results in Figure 4. The error bar in Figure 4 represents the combined depth measurement errors from LA-ICP-MS (±0.5 cm, estimated from possible error in measuring the exact start of the laser line) and the ECM. Annual layers (arrows in Fig. 4) were identified in the LA-ICP-MS profiles by manually selecting winter–spring maximum input peaks in the Na profile (Mayewski and others, 1997). By this approach the LA-ICP-MS chemical profile contains 9 years between 1678.38 and 1678.84 m. Focusing on the most continuous section from 1678.38 to 1678.58 m, the resulting annual-layer thickness is equal to the ~3 cm a^{-1} determined by Meese and others (1997).

The LA-ICP-MS profile of the very deep ice also contains annual layers in the chemical record consistent with original

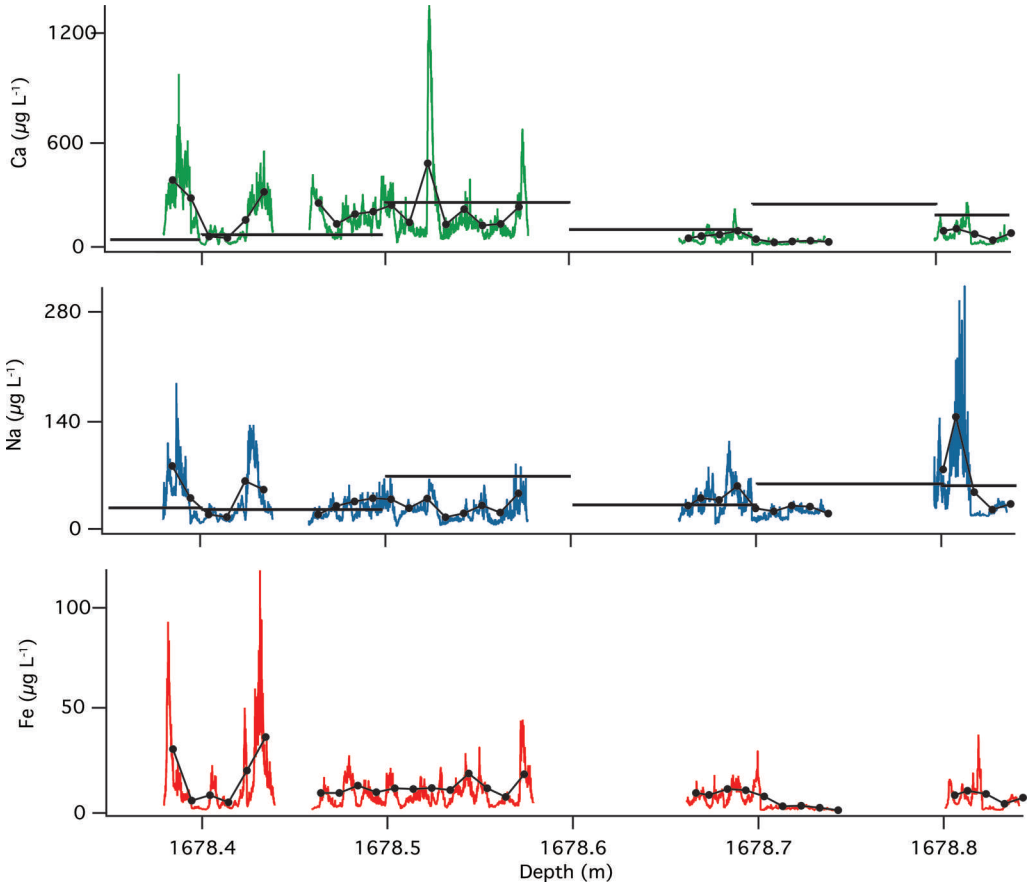

Fig. 6. Smoothed LA-ICP-MS (ten-point running mean) Ca (green), Na (blue) and Fe (red) profiles measured on GISP2 ice core superimposed with simulated 1 cm data (black lines with dots) based on averaging of LA-ICP-MS results. Original Ca^{2+} and Na^{+} measured by IC presented as horizontal bars at 10 cm sample resolution. Arrows indicate annual-layer picks based on Na peaks.

determinations. At 2680 m depth the GISP2 ice core was identified to contain 208 years in this meter of core (~2 years in 1 cm) based on laser-light scattering of ice and stratigraphy (Meese and others, 1997). The LA-derived Ca, Na and Fe raw and ten-point mean smooth profiles of the 10 cm subsection (Fig. 5) indeed show annual-layer picks at 17 years, which is consistent with Meese and others (1997) as annual layers are not uniformly deposited and this represents only 10% of the total meter originally counted.

Comparison of current continuous melter ICP-MS sample resolution and LA-ICP-MS sample resolution

To evaluate what the chemical record might look like using continuous melting techniques, we simulate the 1 cm current state-of-the-art resolution for this technique by averaging the LA-ICP-MS data from 1678 m (dots, Fig. 6). Annual signals are not recognizable at 1 cm resolution or are only represented by one data point, demonstrating that the ultra-fine sample resolution of the laser system is essential to identify annual layers in the chemical record at this and greater depths in the GISP2 ice core. Also presented in Figure 6 are the original Ca^{2+} and Na^{+} (black curves), highlighting the increased sampling resolution achievable with LA.

LA-ICP-MS intensity to chemical concentration calibration

We test our LA-ICP-MS calibration strategy by comparing our results with original concentrations determined by IC (Mayewski and others, 1997) (Fig. 6). GISP2 Ca^{2+} and Na^{+} average concentrations from 1678.4 to 1678.8 m at the original 10 cm sample resolution are 107.8 and 40.4 μg L^{-1} respectively. The average LA-ICP-MS Ca and Na concentrations in the portion from 1678.38 to 1678.84 m are 140.5 and 36.8 μg L^{-1}, respectively. We also compare the original IC concentrations at meter 2680 to the LA-ICP-MS-derived concentrations. At this depth the original sample resolution was 20 cm. The IC Ca^{2+} and Na^{+} results for the sample from 2680.00 to 2680.20 m depth are 95.78 and 30.16 μg L^{-1}, respectively. LA-ICP-MS Ca and Na averages for the range 2680.02 m–2680.12 m are 93.9 and 36.7 μg L^{-1}, respectively.

Comparison between particles, 1 cm depth resolution conductivity and LA-ICP-MS-derived chemical species

We selected a portion of a Colle Gnifetti (Switzerland) ice core collected in 2005 to compare LA-derived results with previously determined meltwater conductivity and particle concentrations. Meltwater conductivity is a measure of total ions in solution. It is measured on meltwater during CFA with an uncertainty in depth resolution of ±1 cm (Röthlisberger and others, 2000) and a conductivity reading error of ±0.2% (Radiometer Analytical, France). Particle concentration is determined by a laser-scattering method also on meltwater (±1 cm depth error) with a size detection limit of ~1 μm diameter (Ruth and others, 2002). We present LA-derived Ca, Na and Fe to examine the possible contributions of these elements to the particle and meltwater conductivity profiles. All three elements may be preserved in ice cores as soluble and insoluble species (De Angelis and others, 1997;

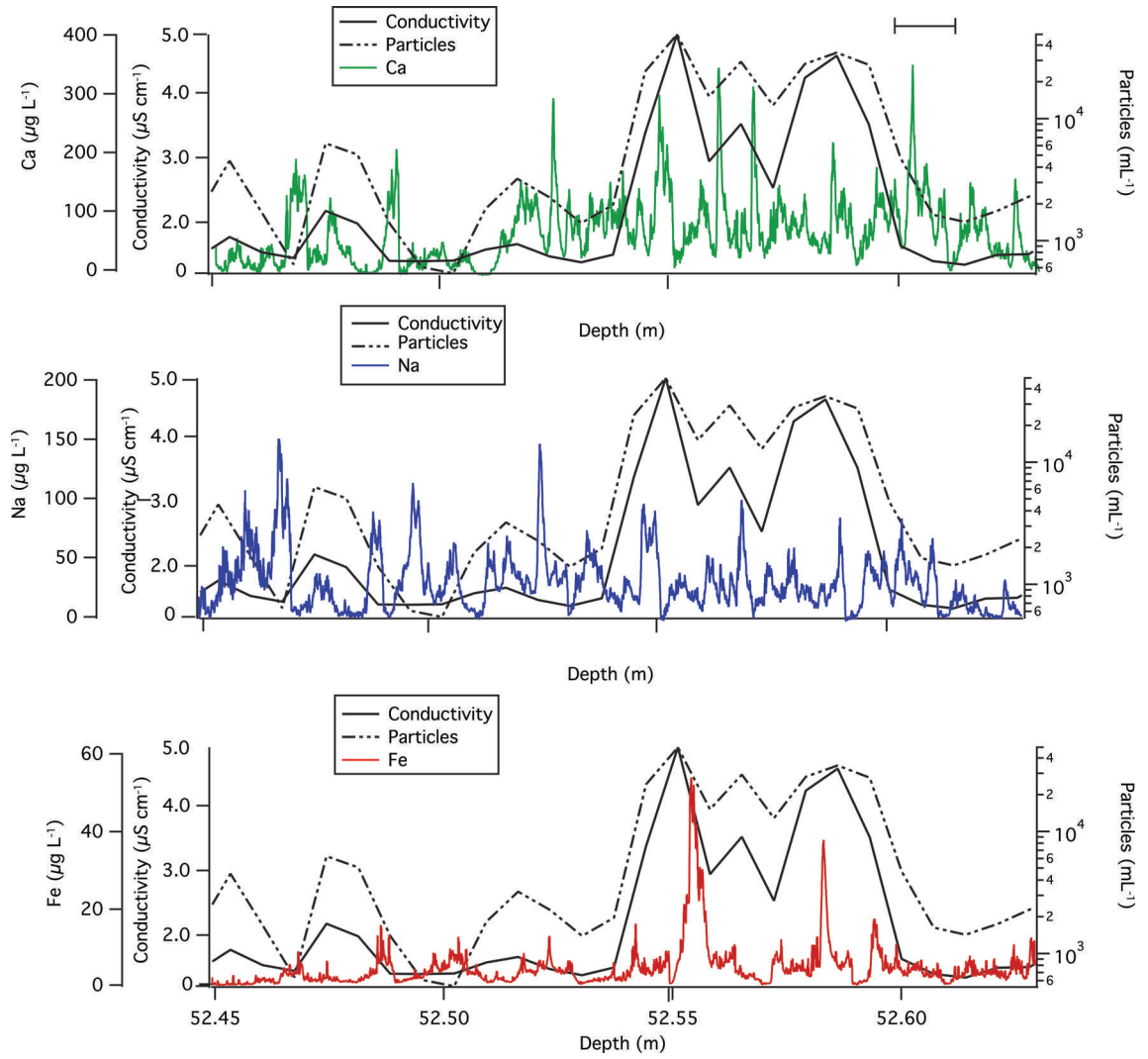

Fig. 7. Results from LA-ICP-MS analyses of the 2003 Colle Gnifetti ice core. Panels show ten-point smooth LA-ICP-MS Ca (green), Na (blue) and Fe (red). Superimposed are cm-resolution CFA data of meltwater conductivity (solid black curve) and particle content (dashed black curve). Error bar represents combined depth error estimates for LA-ICP-MS (±0.5 cm) and CFA (±1.0 cm). LA-ICP-MS detection limits (not shown) are 2.1, 2.3 and 0.1 μg L^{-1} for Ca, Na and Fe respectively, ±0.2% for meltwater conductivity, and particle sizes are >1 μm.

Laj and others, 1997). A comparison of elemental concentrations (μg L^{-1}, ten-point running smooth) determined by LA-ICP-MS (~±2 μg L^{-1}, conservatively estimated from instrument detection limits) with particles and meltwater conductivity appears in Figure 7. The error bar is an estimate of combined depth measurement errors of ±0.5 cm for LA-ICP-MS and ±1 cm for CFA. Particle concentration and meltwater conductivity rise and fall similarly, indicating that peaks in these measurements are made up of both soluble and insoluble material. Fe and Ca display the most covariation with the highest particle and conductivity peaks.

Lastly, using a recently (2013) collected Colle Gnifetti core we compare LA-ICP-MS Ca with the current state-of-the-art CFA Ca^{2+} (Fig. 8). The CFA system is described by Kaufmann and others (2008). Measurements were performed on subsections of the same ice-core segment. The top panel is full-resolution LA-ICP-MS Ca, and the bottom is Ca smoothed to simulate the sample resolution of the CFA data. The results from 47.0 to 47.8 m highlight the excellent agreement between the smoothed LA-ICP-MS signal and CFA Ca, with additional high-frequency information offered by LA-ICP-MS absent in conventional CFA.

CONCLUSIONS

We have developed a laser ablation cryocell (Sayre Cell) for use in ICP-MS analysis, capable of holding and keeping frozen up to 1 m sections of ice core. The new cryocell only requires the section of ice core to have a flat surface 3–8 cm wide, thus minimizing sample preparation compared to standard ice-core melting technologies. In addition, LA-ICP-MS uses minimal sample volume, allowing for replicate sampling and availability of almost the entire original core for other analyses. This is especially beneficial if using this technique to complement traditional analytical methods. Repeated measurements made on a Greenland ice-core segment verify the reproducibility of the LA-ICP-MS measurements and preservation of the chemical profile on a micrometer scale. Also, examination of Greenland ice by LA-ICP-MS reveals structure not previously detected in the lower-resolution original chemical record. During the transition into the Holocene (1678 m) and within the glacial period (2680 m), annual layers are observed in LA-derived Ca, Na and Fe profiles consistent with original annual-layer determinations only by visual stratigraphy, ECM and laser-light scattering. Calibration between LA-ICP-MS measured

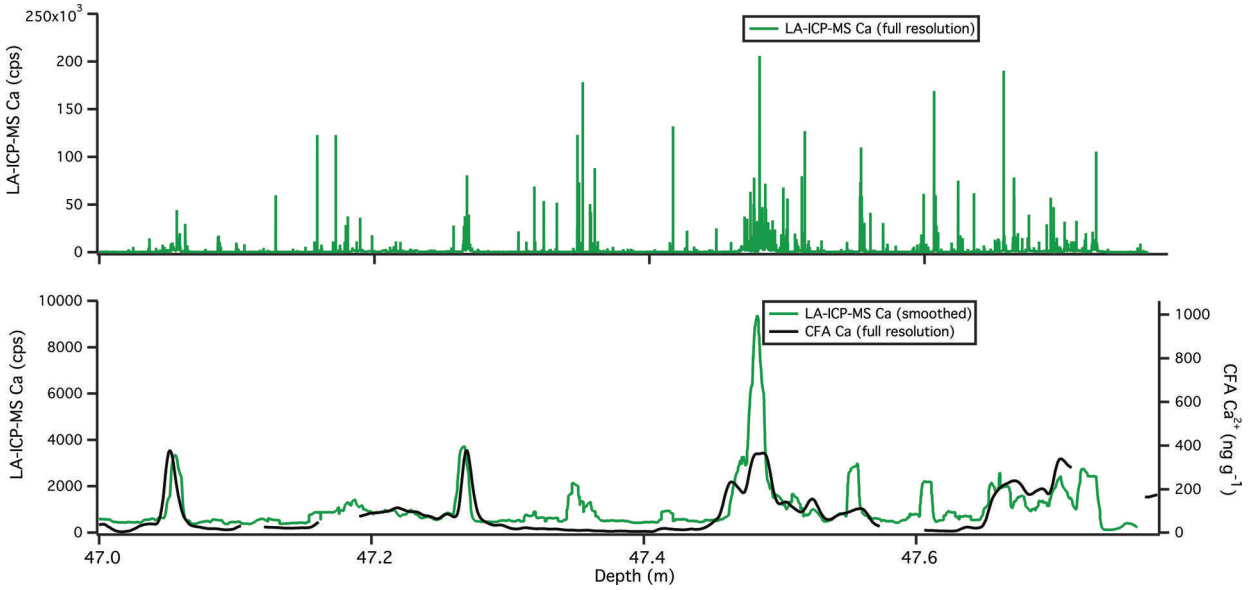

Fig. 8. Comparison of 80 cm of LA-ICP-MS Ca and CFA Ca^{2+}on a Colle Gnifetti ice core collected in 2013 measured on subsections of the same ice-core segment. Top panel is full resolution LA-ICP-MS Ca; bottom LA-ICP-MS is Ca (green) smoothed to simulate the sample resolution of the CFA data (black).

intensity and chemical species concentration is achieved with liquid standards and by ablating a frozen standard reference material to yield a transfer function. The technique is validated through comparison to original IC results. Association of the chemistry contained in the Colle Gnifetti ice core with particle concentration and meltwater conductivity indicates that Ca and Fe display the most covariation species of the three elements measured, possibly due to the mineral origins of Ca and Fe. Lastly, comparison of CFA-derived Ca with LA-ICP-MS Ca demonstrates an outstanding level of agreement plus the inclusion of higher-frequency information in the LA-ICP-MS profile not discernible in the CFA record.

ACKNOWLEDGEMENTS

This work was made possible by a grant from the W.M. Keck Foundation and US National Science Foundation (NSF) grant 1203640. The cryocell was assembled at the University of Maine's Advanced Manufacturing Center. The GISP2 ice core was collected under a grant provided by the NSF. The Colle Gnifetti core was collected with financial support from the Arcadia Foundation and the European Union project ALPCLIM. We acknowledge the Physical Institute of the University of Bern for their invaluable support in the drilling and recovery of the Colle Gnifetti drilling. We also thank the Chief Editor of the *Journal* and two anonymous reviewers for their time and effort, which significantly improved the manuscript.

REFERENCES

Alley RB and 11 others (1997) Visual-stratigraphic dating of the GISP2 ice core: basis, reproducibility, and application. *J. Geophys. Res.*, **102**(C12), 26 367–26 382 (doi: 10.1029/96JC03837)

Bigler M, Svensson A, Kettner E, Vallelonga P, Nielsen ME and Steffensen JP (2011) Optimization of high-resolution continuous flow analysis for transient climate signals in ice cores. *Environ. Sci. Technol.*, **45**(10), 4483–4489 (doi: 10.1021/es200118j)

De Angelis M, Steffensen JP, Legrand M, Clausen H and Hammer C (1997) Primary aerosol (sea salt and soil dust) deposited in Greenland ice during the last climatic cycle: comparison with East Antarctic records. *J. Geophys. Res.*, **102**(C12), 26 681–26 698 (doi: 10.1029/97JC01298)

Gray AL (1985) Solid sample introduction by laser ablation for inductively coupled plasma source mass spectrometry. *Analyst*, **110**(5), 551–556 (doi: 10.1039/AN9851000551)

Guillong M, Horn I and Günther D (2003) A comparison of 266 nm, 213 nm and 193 nm produced from a single solid state Nd: YAG laser for laser ablation ICP-MS. *J. Anal. Atom. Spectrom.*, **18**(10), 1224–1230 (doi: 10.1039/B305434A)

Hamilton WL and Langway CC Jr (1967) A correlation of microparticle concentrations with oxygen isotope ratios in 700 year old Greenland ice. *Earth Planet. Sci. Lett.*, **3**, 363–366 (doi: 10.1016/0012-821X(67)90062-3)

Hammer CU, Clausen HB and Dansgaard W (1981) Past volcanism and climate revealed by Greenland ice cores. *J. Volcan. Geotherm. Res.*, **11**(1), 3–10 (doi: 10.1016/0377-0273(81)90071-8)

Kaspari S and 6 others (2004) Climate variability in West Antarctica derived from annual accumulation-rate records from ITASE firn/ice cores. *Ann. Glaciol.*, **39**, 585–594 (doi: 10.3189/172756404781814447)

Kaufmann PR and 7 others (2008) An improved continuous flow analysis system for high-resolution field measurements on ice cores. *Environ. Sci. Technol.*, **42**(21), 8044–8050 (doi: 10.1021/es8007722)

Laj P and 7 others (1997) Distribution of Ca, Fe, K, and S between soluble and insoluble material in the Greenland Ice Core Project ice core. *J. Geophys. Res.*, **102**(C12), 26 615–26 623 (doi: 10.1029/96JC02660)

Longerich H (2008) Laser ablation–inductively coupled plasma–mass spectrometry (LA–ICP–MS); an introduction. In Sylvester P ed. *Laser ablation ICP-MS in the earth sciences: current practices and outstanding issues*. (Short Course Series 40) Mineralogical Association of Canada, Vancouver, BC, 1–18

Mayewski PA and 6 others (1997) Major features and forcing of high-latitude Northern Hemisphere atmospheric circulation using a 110,000-year-long glaciochemical series. *J. Geophys. Res.*, **102**(C12), 26 345–26 366 (doi: 10.1029/96JC03365)

Meese DA and 8 others (1994) The accumulation record from the GISP2 core as an indicator of climate change throughout the

Holocene. *Science*, **266**(5191), 1680–1682 (doi: 10.1126/science.266.5191.1680)
Meese DA and 8 others (1997) The Greenland Ice Sheet Project 2 depth–age scale: methods and results. *J. Geophys. Res.*, **102**(C12), 26 411–26 423 (doi: 10.1029/97JC00269)
Miller JC (1993) A brief history of laser ablation. *AIP Conf. Proc.*, **288**, 619–622 (doi: 10.1063/1.44865)
Müller W, Shelley M, Miller P and Broude S (2009) Initial performance metrics of a new custom-designed ArF excimer LA-ICPMS system coupled to a two-volume laser-ablation cell. *J. Anal. Atom. Spectrom.*, **24**(2), 209–214 (doi: 10.1039/B805995K)
Müller W, Shelley JMG and Rasmussen SO (2011) Direct chemical analysis of frozen ice cores by UV-laser ablation ICPMS. *J. Anal. Atomic Spectrom.*, **26**(12), 2391–2395 (doi: 10.1039/C1JA10242G)
O'Dwyer J and 7 others (2000) Methanesulfonic acid in a Svalbard ice core as an indicator of ocean climate. *Geophys. Res. Lett.*, **27**(8), 1159–1162 (doi: 10.1029/1999GL011106)
Osterberg EC, Handley MJ, Sneed SB, Mayewski PA and Kreutz KJ (2006) Continuous ice core melter system with discrete sampling for major ion, trace element, and stable isotope analyses. *Environ. Sci. Technol.*, **40**(10), 3355–3361 (doi: 10.1021/es052536w)
Ram M, Illing M, Weber P, Koenig G and Kaplan M (1995) Polar ice stratigraphy from laser-light scattering: scattering from ice. *Geophys. Res. Lett.*, **22**(24), 3525–3527 (doi: 10.1029/95GL03270)
Reinhardt H and 6 others (2001) Laser ablation inductively coupled plasma mass spectrometry: a new tool for trace element analysis in ice cores. *Fresenius' J. Anal. Chem.*, **370**(5), 629–636 (doi: 10.1007/s002160100853)
Reinhardt H, Kriews M, Miller H, Lüdke C, Hoffmann E and Skole J (2003) Application of LA–ICP–MS in polar ice core studies. *Anal. Bioanal. Chem.*, **375**(8), 1265–1275 (doi: 10.1007/s00216-003-1793-5)
Röthlisberger R and 6 others (2000) Technique for continuous high-resolution analysis of trace substances in firn and ice cores. *Environ. Sci. Technol.*, **34**(2), 338–342 (doi: 10.1021/es9907055)
Russo RE, Mao X, Liu H, Gonzalez J and Mao SS (2002) Laser ablation in analytical chemistry – a review. *Talanta*, **57**(3), 425–451 (doi: 10.1016/S0039-9140(02)00053-X)
Ruth U, Wagenbach D, Bigler M, Steffensen JP, Röthlisberger R and Miller H (2002) High-resolution microparticle profiles at NorthGRIP, Greenland: case studies of the calcium–dust relationship. *Ann. Glaciol.,* **35**, 237–242 (doi: 10.3189/172756402781817347)
Tadano J, Kumakura H and Ito Y (2004) Coupling of focused laser pulse to surfaces of transparent materials studied by time-resolved imaging technique. *Appl. Phys. A.*, **79**(4–6), 1031–1033 (doi: 10.1007/s00339-004-2621-2)
Taylor K and 6 others (1992) Ice-core dating and chemistry by direct-current electrical conductivity. *J. Glaciol.*, **38**(130), 325–332
Taylor KC and 9 others (1993) Electrical conductivity measurements from the GISP2 and GRIP Greenland ice cores. *Nature*, **366**(6455), 549–552 (doi: 10.1038/366549a0)
Taylor KC, Alley RB, Lamorey GW and Mayewski PA (1997) Electrical measurements on the Greenland Ice Sheet Project 2 core. *J. Geophys. Res.*, **102**(C12), 26 511–26 517 (doi: 10.1029/96JC02500)
Wagenbach D, Münnich KO, Schotterer U and Oeschger H (1988) The anthropogenic impact on snow chemistry at Colle Gnifetti, Swiss Alps. *Ann. Glaciol.,* **10**, 183–187
Warren SG and Brandt RE (2008) Optical constants of ice from the ultraviolet to the microwave: a revised compilation. *J. Geophys. Res.*, **113**(D14), D14220 (doi: 10.1029/2007JD009744)
Zielinski GA, Mayewski PA, Meeker LD, Whitlow SI and Twickler MS (1996) 110,000-yr record of explosive volcanism from the GISP2 (Greenland) ice core. *Quat. Res.*, **45**(2), 109–118 (doi: 10.1006/qres.1996.0013)

MS received 23 July 2014 and accepted in revised form 7 January 2015